Acta Cryst. (1979). B**35**, 867–877

A Study of the Charge Density in Putrescine Diphosphate at 85 K*

BY FUSAO TAKUSAGAWA AND THOMAS F. KOETZLE†

Chemistry Department, Brookhaven National Laboratory, Upton, New York 11973, *USA*

(*Received* 15 *March* 1978; *accepted* 7 *September* 1978)

Abstract

A study of the charge density in putrescine diphosphate $\{C_4H_{14}N_2^{2+}.2H_2PO_4^-$, $[NH_3(CH_2)_4NH_3]^{2+}.2[H_2PO_4]^-\}$ has been carried out, employing X-ray and neutron diffraction data measured at a temperature of 85 K. Crystal data: space group $P2_1/a$; $a = 7{\cdot}879$ (3), $b = 9{\cdot}734$ (4), $c = 8{\cdot}126$ (3) Å, $\beta = 110{\cdot}19$ (9)° (X-ray values); $Z = 2$. The deformation electron density was computed by a modified *X–N* method, utilizing neutron positional parameters for all atoms and thermal parameters for non-hydrogen atoms taken from a high-order X-ray refinement ($0{\cdot}65 \leq \sin\theta/\lambda \leq 1{\cdot}15$ Å^{-1}). This approach was elected, since the neutron thermal parameters were found to be systematically larger than those from high-order X-ray refinements. In the case of H atoms, the neutron thermal parameters were multiplied by the mean ratio of the X-ray and neutron values, computed separately for each U_{ij} class for the non-hydrogen atoms. These ratios for the high-order X-ray refinements range from 0·86 to 0·99. Well-defined peaks (0·25–0·35 e Å^{-3}) are found in the deformation density maps for all covalent bonds in the structure. No marked difference was observed between the density in P—O bonds and that in bonds between first-row elements. In the hydrogen bonds, no build up of charge was observed midway between the protons and oxygen acceptors, in accord with the basic electrostatic picture of hydrogen-bonded interactions. Excess density was observed in the regions normally associated with lone-pair electrons for all four phosphate O atoms, and the heights of these peaks increased more than those of peaks in covalent bonds when higher-order data were included in the deformation maps. Conformations of $H_2PO_4^-$ ions in a number of crystal structures including putrescine diphosphate were generally found to have H—O—P—O(H) torsion angles in the range 30–150°; such conformations are predicted to be favored for systems like $H_2PO_4^-$ with lone-pair electrons adjacent to polar bonds.

* Research carried out at Brookhaven National Laboratory under contract with the US Department of Energy and supported by its Office of Basic Energy Sciences.

† To whom correspondence should be addressed.

Introduction

Recent improvements of the precision attainable in single-crystal diffraction measurements have led to increased interest in the direct analysis of charge-density distributions in solids based on diffraction techniques (Coppens, 1975). Here we report a study of the electron density in putrescine diphosphate at 85 K, using combined X-ray and neutron diffraction data. This compound initially attracted our attention, because it affords the opportunity to study the charge density in the dihydrogen phosphate anion, and exhibits a variety of N—H···O and O—H···O hydrogen bonds involving the ammonium groups on putrescine and the phosphate O atoms. The crystal structure was originally determined from X-ray photographic data at room temperature (Woo & Rich, 1975; Woo, Seeman & Rich, 1979). These authors have described the general features of the structure, and commented on its significance as a model for understanding interactions of amines with nucleic acids. Our neutron diffraction results have been described in a previous paper (Takusagawa & Koetzle, 1978).

Experimental

The sample of putrescine diphosphate used in the present X-ray work was recrystallized from an aqueous solution of putrescine and phosphoric acid. A crystal was ground to form a sphere of diameter 0·42 mm which was glued to an aluminum fiber with adhesive varnish‡ and oriented approximately along the crystallographic *c* axis. This sample was placed in a liquid-nitrogen-cooled cryostat (Coppens *et al.*, 1974) and mounted on an automated Picker four-circle diffractometer (Dimmler, Greenlaw, Kelley, Potter, Rankowitz & Stubblefield, 1976; McMullan, Andrews, Koetzle, Reidinger, Thomas & Williams, 1976). Nb-filtered Mo $K\alpha$ radiation ($\lambda = 0{\cdot}71069$ Å) was used. The temperature of a copper block in the cryostat, maintained in direct contact with the aluminum crystal mount, was measured to be 85 ± 1 K during the period

‡ General Electric No. 7031.

of data collection. Cell dimensions refined by a least-squares procedure based on the setting angles of 29 reflections ($2\theta \geq 80°$) (Mo $K\alpha_1$: $\lambda = 0{\cdot}70926$ Å) are listed along with certain experimental details and are compared with the corresponding neutron values in Table 1. X-ray intensities were measured for reflections in four octants of reciprocal space (hkl, $\bar{h}kl$, $h\bar{k}l$, and $\bar{h}\bar{k}l$), out to a 2θ limit of 110°. Mechanical constraints introduced by the cryostat prevented the measurement of reflections with χ near 90° and $2\theta > 70°$, but the number of reflections omitted was a small fraction of the total data measured. A $\theta/2\theta$ step-scan procedure was used; the scan range varied from 3·0 to 3·5° over the full range of 2θ, while the step size was taken to be $\Delta 2\theta = 0{\cdot}04°$. At each step, counts were accumulated for 2 s. As a general check on experimental stability, the intensities of two reflections were remeasured every 30 reflections. These intensities did not vary to any significant degree during the course of the measurements.

Integrated intensities were obtained with the program *PEAK* (Takusagawa, 1977) written for a PDP 11/40 computer equipped with an interactive CRT display (Bernstein *et al.*, 1974; Vector General, Inc., 1973). A profile analysis was carried out for strong reflections with $I > 15\sigma(I)$, and the resulting peak widths were fitted by a least-squares procedure with a function of the type: $\Delta\theta = Ax + B$, $x = [2(\lambda_2 - \lambda_1)/(\lambda_1 + \lambda_2)] \tan\theta$, where λ_1 (0·7093 Å) and λ_2 (0·7136 Å) are the wavelengths of Mo $K\alpha_1$ and Mo $K\alpha_2$, respectively. A and B were determined to be 1·99 and 1·06°, respectively, based on approximately 12 000 strong reflections. Calculated values of $\Delta\theta$ range from 1·06 to 1·45° for $0 < 2\theta < 110°$. The peak-width function defined above was used to determine trial points for the separation of peak and background regions in each individual scan. Final delineation of backgrounds was accomplished by the method of Lehmann & Larsen (1974). At various points in the integration process, it was possible to examine selected profiles on the CRT, and certain reflections with unusual profiles were integrated manually.

Intensity data for several reflections collected as a function of rotation about the scattering vector indicated 2–3% variation in absorption. Therefore, observed intensities were corrected for absorption by a semi-empirical method (North, Phillips & Mathews, 1968), based upon these ψ-scan measurements. Observed squared structure factors were calculated as $F_o^2 = 2I \sin 2\theta/(1 + \cos^2 2\theta)$ and averaged for symmetry-related reflections. The agreement factor obtained is

$$R_c = \sum_{hkl} \langle \Delta F_o^2 \rangle / \sum_{hkl} \langle F_o^2 \rangle = 0{\cdot}022;$$

$$\langle \Delta F_o^2 \rangle = \sum_{i=1}^{n} | \langle F_o^2 \rangle - F_{oi}^2 | /n,$$

where n is the number of observations for a given reflection hkl and its symmetry equivalents. The standard deviation of each reflection was estimated as follows: $\sigma^2(F_o^2) = \sigma^2(\text{count}) + (AF_o^2)^2 + (BF_o^4)^2$. Constants A and B were determined from $\langle \Delta F_o^2 \rangle$ by a least-squares procedure minimizing the quantity $\sum_{hkl} [\langle \Delta F_o^2 \rangle - \sigma^2(F_o^2)]^2$. The resulting values are $A = 1{\cdot}34 \times 10^{-2}$ and $B = 2{\cdot}46 \times 10^{-8}$.

Table 1. *Crystal data for putrescine diphosphate* ($T = 85$ K)

$C_4H_{14}N_2^{2+}.2H_2PO_4^-$, FW 284·14

	X-ray	Neutron
a	7·879 (3) Å	7·890 (7) Å
b	9·734 (4)	9·725 (8)
c	8·126 (3)	8·132 (8)
β	110·19 (9)°	110·26 (5)°
V	584·9 Å³	585·4 Å³
Space group	$P2_1/a$	$P2_1/a$
ρ_c	1·614 Mg m⁻³	1·613 Mg m⁻³
Crystal volume	0·039 mm³	7·75 mm³
$(\sin\theta/\lambda)_{max}$	1·153 Å⁻¹	0·675 Å⁻¹
Total number of reflections	16767	3208
Unique reflections	6840	1691
Absorption coefficient	40·85 mm⁻¹	23·48 mm⁻¹
Transmission range	0·840 ~ 0·864	0·801 ~ 0·870

X-ray refinements

Initial positional parameters for all atoms were fixed at values determined in the neutron diffraction study (Takusagawa & Koetzle, 1978). X-ray scattering factors for P, O, N and C atoms were taken from the relativistic Hartree–Fock values given in *International Tables for X-ray Crystallography* (1974); those for H atoms were from Stewart, Davidson & Simpson (1965). For non-hydrogen atoms, the anomalous-dispersion factors of Cromer & Liberman (1970) were applied. A type I isotropic extinction correction (Becker & Coppens, 1974) was included in the refinements. The minimum extinction correction factor is $y = 0{\cdot}25$ (y divides F_o^2) for the 001 reflection.

Conventional and high-order X-ray refinements were carried out, as described in detail in Table 2. Procedures 1–5 are 'pure' X-ray refinements, in which isotropic thermal parameters were assigned to H atoms and anisotropic thermal parameters to non-hydrogen atoms. In procedures 6 and 7, positional parameters of all atoms and anisotropic thermal parameters of H atoms were fixed to the neutron values. The results of procedure 7 were used to calculate the deformation density, after suitable modification of the H-atom thermal parameters, as described below. Atomic parameters obtained in the conventional X-ray refine-

Table 2. *Details of refinements*

All calculations are full-matrix least-squares refinements, utilizing only reflections with $F_o^2 > 3\sigma(F_o^2)$. The quantity minimized is $\Sigma\, w(F_o^2 - k^2 F_c^2)^2$, where $w = 1/\sigma^2(F_o^2)$.

Procedure	(sin θ/λ) range (Å^{-1})	N_o	N_v	$R(F^2)$	$wR(F^2)$	S*	Scale (k)	Maximum correlation
1	0·00–1·15	6258	110	0·027	0·025	1·91	15·31 (1)	0·68
2	0·65–1·15	4975	73†	0·033	0·029	1·81	15·38 (2)	0·63
3	0·85–1·15	3463	72†	0·043	0·037	1·83	15·38§	0·70
4	1·00–1·15	1881	72†	0·052	0·043	1·87	15·38§	0·62
5	0·00–0·65	1281	110	0·013	0·017	2·10	15·22 (4)	0·79
6	0·00–1·15	6258	50‡	0·029	0·026	2·05	15·33 (1)	0·68
7	0·65–1·15	4975	49‡¶	0·035	0·031	1·89	15·39 (2)	0·63

* $S = [\Sigma\, w(F_o^2 - k^2F_c^2)^2/(N_o - N_v)]^{1/2}$, where N_o = number of observations, and N_v = number of variables.

† Positional and isotropic thermal parameters for hydrogen atoms and the extinction parameter were taken from the results of refinement 2.

‡ All positional parameters and anisotropic thermal parameters for hydrogen atoms were fixed to the neutron results. Other parameters were refined.

§ Not varied.

¶ The extinction parameter was fixed to the results of refinement 6.

Table 3. *Fractional atomic coordinates and thermal parameters*

N = Neutron data. $X1$ = X-ray data ($0{\cdot}00 \le \sin\theta/\lambda \le 1{\cdot}15$ Å^{-1}). $X2$ = X-ray data ($0{\cdot}65 \le \sin\theta/\lambda \le 1{\cdot}15$ Å^{-1}). $X3$ = X-ray data ($0{\cdot}85 \le \sin\theta/\lambda \le 1{\cdot}15$ Å^{-1}). The anisotropic Debye–Waller factor is of the form $\exp[-2\pi^2(h^2a^{*2}U_{11} + \cdots + 2hka^*b^*U_{12} + \cdots)]$.

		x	y	z	U_{11}	U_{22}	U_{33}	U_{12}	U_{13}	U_{23}
P	N	0·84554 (11)	1·112562 (68)	0·120702 (85)	0·00625 (34)	0·00546 (25)	0·00752 (27)	−0·00010 (23)	0·00388 (21)	0·00055 (21)
	$X1$	0·845608 (11)	1·112566 (8)	0·120753 (11)	0·005604 (23)	0·005893 (23)	0·006304 (28)	−0·000122 (17)	0·003051 (18)	0·000391 (18)
	$X2$	0·845613 (12)	1·112558 (9)	0·120758 (12)	0·005677 (25)	0·005958 (26)	0·006398 (31)	−0·000111 (18)	0·003092 (19)	0·000396 (18)
	$X3$	0·845613 (16)	1·112554 (12)	0·120760 (17)	0·005722 (24)	0·005967 (24)	0·006425 (32)	−0·000113 (22)	0·003107 (21)	0·000404 (23)
O(1)	N	0·66424 (10)	1·118495 (66)	0·143343 (84)	0·00855 (31)	0·00893 (24)	0·01389 (27)	0·00103 (22)	0·00696 (20)	0·00061 (21)
	$X1$	0·663971 (31)	1·118484 (24)	0·143367 (34)	0·007566 (61)	0·008792 (65)	0·012241 (84)	0·001070 (50)	0·006168 (57)	0·000716 (55)
	$X2$	0·664019 (34)	1·118506 (27)	0·143356 (38)	0·007619 (62)	0·008799 (66)	0·012252 (87)	0·001043 (51)	0·006144 (58)	0·000672 (57)
	$X3$	0·664068 (43)	1·118508 (35)	0·143375 (51)	0·007685 (70)	0·008820 (76)	0·01238 (11)	0·001036 (60)	0·006198 (69)	0·000704 (68)
O(2)	N	0·838771 (97)	1·137247 (64)	0·066036 (78)	0·00893 (32)	0·00843 (24)	0·00822 (23)	0·00027 (21)	0·00434 (19)	0·00058 (19)
	$X1$	0·838693 (31)	1·137359 (23)	0·066113 (31)	0·008231 (61)	0·008454 (61)	0·006522 (71)	0·000473 (48)	0·003541 (51)	0·000586 (47)
	$X2$	0·838687 (34)	1·137344 (25)	−0·066098 (34)	0·008277 (62)	0·008557 (62)	0·006524 (74)	0·000445 (48)	0·003539 (51)	0·000554 (48)
	$X3$	0·838709 (43)	1·137312 (32)	−0·066013 (47)	0·008331 (71)	0·008544 (71)	0·006703 (92)	0·000419 (56)	0·003631 (61)	0·000533 (57)
O(3)	N	0·97695 (12)	1·216356 (81)	0·248778 (89)	0·01788 (38)	0·01918 (32)	0·00987 (25)	−0·01107 (27)	0·00630 (23)	0·00359 (23)
	$X1$	0·976922 (42)	1·216363 (32)	0·249246 (36)	0·016547 (98)	0·01812 (10)	0·008416 (87)	−0·010753 (81)	0·005208 (71)	−0·003405 (69)
	$X2$	0·976923 (52)	1·216374 (40)	0·249288 (43)	0·01653 (10)	0·01807 (11)	0·008420 (92)	0·010613 (87)	0·005172 (75)	0·003347 (72)
	$X3$	0·976962 (73)	1·216285 (57)	0·249295 (63)	0·01661 (13)	0·01810 (14)	0·00845 (12)	−0·01053 (11)	0·005223 (95)	0·003315 (91)
O(4)	N	0·92057 (11)	0·964394 (71)	0·182925 (91)	0·01470 (37)	0·01126 (26)	0·01687 (29)	0·00598 (25)	0·01067 (23)	0·00583 (23)
	$X1$	0·920264 (38)	0·964186 (27)	0·182856 (39)	0·013908 (84)	0·010358 (73)	0·015590 (97)	0·005920 (62)	0·009957 (74)	0·005934 (65)
	$X2$	0·920199 (45)	0·964177 (31)	0·182756 (47)	0·013916 (88)	0·010430 (75)	0·01554 (11)	0·005873 (65)	0·009879 (80)	0·005887 (69)
	$X3$	0·920105 (61)	0·964142 (43)	0·182566 (67)	0·01389 (11)	0·010465 (90)	0·01552 (14)	0·005813 (81)	0·00982 (10)	0·005871 (87)
N	N	0·552751 (61)	0·868790 (41)	0·232165 (49)	0·00896 (20)	0·00818 (16)	0·00879 (16)	−0·00019 (14)	0·00403 (12)	−0·00086 (12)
	$X1$	0·552758 (35)	0·868816 (25)	0·232226 (35)	0·008307 (68)	0·007953 (68)	0·006836 (79)	0·000071 (51)	0·002998 (56)	−0·000694 (51)
	$X2$	0·552796 (37)	0·868797 (27)	0·232218 (38)	0·008365 (68)	0·008043 (69)	0·006865 (81)	0·000097 (51)	0·003007 (57)	−0·000689 (51)
	$X3$	0·552838 (48)	0·868800 (34)	0·232232 (52)	0·008436 (78)	0·008031 (81)	0·00707 (10)	−0·000074 (59)	0·003134 (69)	0·000748 (61)
C(1)	N	0·634888 (90)	0·857174 (59)	0·426793 (71)	0·01164 (30)	0·01037 (22)	0·00918 (21)	0·00291 (20)	0·00362 (18)	0·00003 (17)
	$X1$	0·634972 (43)	0·857295 (33)	0·426771 (41)	0·011145 (91)	0·010084 (85)	0·007054 (96)	0·002947 (69)	0·002631 (72)	0·000210 (65)
	$X2$	0·634892 (48)	0·857290 (36)	0·426688 (45)	0·011187 (92)	0·010027 (86)	0·00730 (10)	0·002920 (70)	0·002727 (73)	0·000214 (66)
	$X3$	0·634888 (63)	0·857266 (48)	0·426693 (64)	0·01129 (11)	0·01010 (10)	0·00756 (13)	0·002955 (85)	0·002852 (91)	0·000196 (80)
C(2)	N	0·600127 (88)	0·985279 (60)	0·518474 (69)	0·01010 (30)	0·01144 (23)	0·00934 (23)	0·00080 (20)	0·00328 (18)	−0·00213 (18)
	$X1$	0·600205 (42)	0·985181 (32)	0·518441 (41)	0·009065 (82)	0·010904 (89)	0·007777 (94)	0·000759 (67)	0·002278 (68)	−0·002117 (67)
	$X2$	0·600226 (46)	0·985189 (35)	0·518443 (45)	0·009086 (83)	0·010936 (91)	0·007819 (98)	0·000768 (67)	0·002225 (69)	−0·002062 (67)
	$X3$	0·600208 (59)	0·985169 (47)	0·518438 (63)	0·009124 (97)	0·01093 (11)	0·00786 (13)	0·000782 (80)	0·002218 (84)	−0·002014 (82)
H(1)	N	0·59005 (20)	0·96205 (13)	0·18963 (16)	0·02459 (73)	0·01692 (50)	0·02193 (53)	−0·00257 (46)	0·01020 (44)	0·00265 (41)
	$X1$	0·5903 (17)	0·9521 (11)	0·1936 (16)	0·0281 (25)					
H(2)	N	0·41274 (20)	0·86459 (15)	0·18750 (17)	0·01491 (65)	0·02632 (58)	0·02204 (54)	0·00044 (50)	0·00529 (42)	−0·00058 (47)
	$X1$	0·4254 (15)	0·8622 (11)	0·1919 (15)	0·0232 (23)					
H(3)	N	0·59604 (22)	0·79072 (14)	0·16892 (17)	0·02714 (77)	0·01995 (53)	0·02128 (54)	0·00476 (49)	0·01112 (46)	−0·00512 (43)
	$X1$	0·5900 (17)	0·7988 (12)	0·1725 (15)	0·0277 (25)					
H(4)	N	0·57892 (25)	0·76570 (14)	0·46777 (19)	0·04140 (98)	0·01780 (54)	0·02693 (62)	−0·00175 (56)	0·01649 (57)	0·00428 (47)
	$X1$	0·5809 (16)	0·7723 (11)	0·4641 (15)	0·0215 (23)					
H(5)	N	0·78007 (22)	0·84265 (18)	0·45923 (19)	0·01715 (73)	0·03765 (76)	0·02626 (61)	0·00938 (57)	0·00368 (47)	−0·00316 (54)
	$X1$	0·7714 (14)	0·8444 (11)	0·4549 (14)	0·0216 (20)					
H(6)	N	0·67068 (23)	0·96866 (17)	0·65932 (17)	0·02599 (77)	0·03700 (72)	0·01505 (52)	0·00728 (61)	0·00204 (44)	−0·00355 (50)
	$X1$	0·6658 (15)	0·9674 (11)	0·6504 (16)	0·0215 (23)					
H(7)	N	0·66397 (24)	1·07422 (15)	0·48010 (21)	0·02660 (86)	0·02127 (55)	0·03565 (72)	0·00585 (53)	0·01553 (56)	0·00322 (51)
	$X1$	0·6629 (15)	1·0619 (13)	0·4813 (14)	0·0294 (23)					
H(8)	N	1·05599 (20)	1·27515 (14)	0·20139 (17)	0·02066 (69)	0·02275 (57)	0·02276 (54)	−0·00614 (49)	0·00955 (44)	0·00094 (44)
	$X1$	1·0528 (15)	1·2728 (11)	0·2035 (15)	0·0243 (24)					
H(9)	N	1·01680 (21)	0·93124 (14)	0·13728 (18)	0·02112 (74)	0·02183 (55)	0·02648 (59)	0·00605 (48)	0·01321 (47)	0·00361 (45)
	$X1$	1·0044 (16)	0·9373 (13)	0·1427 (14)	0·0288 (25)					

ment (procedure 1),* and in the refinements based on reflections with $\sin\theta/\lambda \geq 0{\cdot}65$ Å^{-1} (procedure 2) and $\sin\theta/\lambda \geq 0{\cdot}85$ Å^{-1} (procedure 3) are compared with the neutron values in Table 3.

Discussion of the structure

The structure of putrescine diphosphate is shown in Fig. 1, which emphasizes the approximately tetrahedral arrangement of dihydrogen phosphate anions about the ammonium groups of putrescine. The packing exhibits three distinct N–H···O and two O–H···O hydrogen-bonded interactions; atom O(1) accepts two hydrogen bonds, while O(2) accepts three. This structure has been described in some detail in earlier papers (Woo *et al.*, 1979; Takusagawa & Koetzle, 1978). Here we make some comments comparing results of the 85 K X-ray and neutron refinements. Bond distances and angles calculated from the atomic coordinates obtained in the conventional X-ray refinement are given in Table 4 along with the corresponding values from the neutron study. The agreement is in general quite good, except in the case of bond distances involving H, which as expected are systematically short in the X-ray determination.

* A list of structure factors has been deposited with the British Library Lending Division as Supplementary Publication No. SUP 33945 (39 pp.). Copies may be obtained through The Executive Secretary, International Union of Crystallography, 5 Abbey Square, Chester CH1 2HU, England.

Positional parameters

The differences between the positions of non-hydrogen atoms found in the neutron study and those from X-ray refinements (1–5) are given in Table 5 (X-ray asphericity shifts). The C, N and O atoms show significant shifts in the low-order refinement (5),

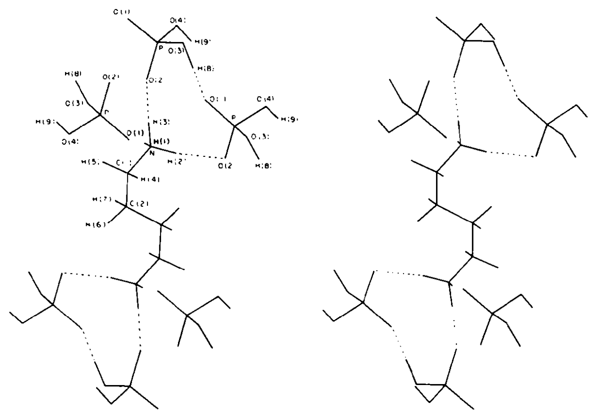

Fig. 1. Schematic stereoscopic representation of the crystal structure of putrescine diphosphate.

Table 4. *Bond distances* (Å) *and angles* (°)

	X-ray*	Neutron		X-ray*	Neutron		X-ray*	Neutron
P–O(1)	1·5056 (6)	1·5030 (13)	C(2)–C(2′)	1·5296 (8)	1·5280 (12)	C(1)–H(5)	1·03 (1)	1·091 (2)
P–O(2)	1·5198 (6)	1·5190 (11)	N–H(1)	0·95 (1)	1·049 (2)	C(2)–H(6)	1·03 (1)	1·098 (1)
P–O(3)	1·5607 (7)	1·5595 (12)	N–H(2)	0·94 (1)	1·036 (2)	C(2)–H(7)	1·00 (1)	1·099 (2)
P–O(4)	1·5754 (6)	1·5745 (11)	N–H(3)	0·94 (1)	1·039 (2)	O(3)–H(8)	0·97 (1)	1·015 (2)
N–C(1)	1·4915 (9)	1·4921 (10)	C(1)–H(4)	1·02 (1)	1·095 (2)	O(4)–H(9)	0·87 (1)	1·005 (2)
C(1)–C(2)	1·5233 (7)	1·5251 (10)						
O(1)–P–O(2)	114·08 (5)	114·14 (7)	C(1)–N–H(2)	112·5 (8)	112·8 (1)	C(2)–C(1)–H(5)	110·0 (6)	109·8 (1)
O(1)–P–O(3)	109·40 (3)	109·48 (7)	C(1)–N–H(3)	113·2 (7)	111·88 (8)	H(4)–C(1)–H(5)	110·2 (9)	108·7 (1)
O(1)–P–O(4)	105·16 (2)	105·26 (6)	H(1)–N–H(2)	111 (1)	107·7 (1)	C(1)–C(2)–H(6)	105·1 (6)	106·1 (1)
O(2)–P–O(3)	110·64 (4)	110·52 (7)	H(1)–N–H(3)	105 (1)	107·0 (1)	C(1)–C(2)–H(7)	105·8 (7)	109·2 (1)
O(2)–P–O(4)	110·26 (2)	110·22 (6)	H(2)–N–H(3)	105 (1)	106·8 (1)	C(2′)–C(2)–H(6)	110·4 (8)	110·5 (1)
O(3)–P–O(4)	106·93 (4)	106·85 (6)	N–C(1)–H(4)	107·6 (6)	108·12 (9)	C(2′)–C(2)–H(7)	112·6 (7)	109·8 (1)
N–C(1)–C(2)	111·79 (3)	111·75 (5)	N–C(1)–H(5)	106·5 (6)	107·5 (1)	P–O(3)–H(8)	117·5 (7)	117·7 (1)
C(1)–C(2)–C(2′)	113·95 (4)	113·87 (5)	C(2)–C(1)–H(4)	110·6 (7)	110·9 (1)	P–O(4)–H(9)	113·7 (8)	115·0 (1)
C(1)–N–H(1)	110·1 (7)	110·28 (8)						

* Results of procedure 1.

Table 5. *X-ray asphericity shifts* (10^{-4} Å)

Procedure	($\sin\theta/\lambda$) range (Å^{-1})	P	O(1)	O(2)	O(3)	O(4)	N	C(1)	C(2)
1	0·00–1·15	6 (4)	22 (9)	13 (7)	39 (9)	30 (9)	5 (5)	14 (7)	12 (7)
2	0·65–1·15	6 (4)	18 (9)	12 (7)	42 (9)	35 (9)	5 (4)	14 (7)	13 (7)
3	0·85–1·15	6 (4)	15 (9)	9 (8)	44 (10)	44 (8)	6 (5)	12 (8)	14 (8)
4	1·00–1·15	5 (5)	20 (9)	16 (9)	56 (13)	62 (9)	5 (9)	8 (11)	12 (11)
5	0·00–0·65	5 (4)	34 (10)	29 (8)	43 (10)	43 (10)	22 (9)	20 (11)	16 (10)

reflecting the contribution of valence electrons. By contrast, the P-atom shift is negligible, as expected due to its tetrahedral environment and the dominant influence of core electrons for a second-row element. In the high-order refinements (2,3,4), shifts are reduced to the 2σ level or below for all non-hydrogen atoms, with the exception of O(3) and O(4), the two protonated O atoms in the $H_2PO_4^-$ ion. These latter shifts are of magnitude 0·004–0·006 Å, and lie in the direction of the expected lone-pair region on each O atom, thus causing relatively minor changes in P—O distances (Table 6). Evidently, asphericity of the valence shell of O(3) and O(4) contributes significantly to reflections beyond $(\sin \theta/\lambda) = 0{\cdot}65$ Å^{-1}. Theoretical evidence for such an effect has been given by Dawson (1964) and Coppens (1969), and the effect has been observed experimentally in sulfamic acid (Bats, Coppens & Koetzle, 1977). It is, however, a little surprising that in the present work the asphericity shifts of O(3) and O(4) are observed to increase marginally upon raising the $(\sin \theta/\lambda)$ cut-off from 0·65 Å^{-1} (procedure 2) to 1·00 Å^{-1} (procedure 4), rather than decreasing as one might expect, while O(1) and O(2) show no significant shifts, except in the low-order refinement (5).

Thermal parameters

Thermal parameters from the present X-ray refinements generally are systematically smaller than those found in the neutron study (Takusagawa & Koetzle, 1978).* The ratios of X-ray and neutron U_{ij}'s determined by least squares for the various X-ray refinements are given in Table 7. There is little difference among the ratios determined for conventional and high-order refinements; depending upon the U_{ij} class, X-ray parameters average from 1–14% lower than the corresponding neutron values. Systematic discrepancies between X-ray and neutron thermal parameters have been observed in a number of other crystals, *e.g.* ammonium tetraoxalate (Stevens, 1973; Currie, Speakman & Curry, 1967), barbital II (Fox, Craven & McMullan, 1977), α-glycylglycine (Griffin & Coppens, 1975; Kvick, Koetzle & Stevens, 1979), parabanic acid (Fox, Craven & McMullan, 1977), sodium azide (Stevens & Hope, 1977; Choi & Prince, 1976), and sulfamic acid (Bats *et al.*, 1977). In ammonium tetraoxalate, α-glycylglycine, sodium azide and sulfamic acid, some thermal parameters in the high-order X-ray refinements were always higher than the corresponding neutron values, contrary to the situation in parabanic acid, barbital II and in the present work on putrescine diphosphate, where the X-ray thermal parameters were found to be lower than the neutron parameters. The origin of these differences is at present not well understood. They could in some cases partly be due to failure to adequately match the temperatures of the X-ray and neutron experiments, but this is considered unlikely in the present work, since the samples used in both experiments were mounted directly on metal pins. At any rate, a temperature difference would produce a constant ratio for all U_{ij} values (Coppens & Vos, 1971) whereas the ratios in Table 7 show significant variation depending upon U_{ij} class. It is interesting to note that the ratio departing furthest from unity is U_{33}, and that the crystal was mounted along the c axis in the X-ray experiment, and along $[10\bar{1}]$ in the neutron experiment. One probable source of error in the thermal parameters stems from thermal diffuse scattering (TDS), which has been shown to exert significant influence on refined thermal parameters, for the X-ray case (Helmholdt & Vos, 1977). Neglect of TDS corrections would be expected to cause the thermal parameters to be smaller than their true values, and TDS might affect the X-ray and neutron experiments to a different extent.

* See previous footnote.

The deformation density

A deformation electron-density map calculated from the observed X-ray structure factors with positional

Table 7. *Ratios of X-ray and neutron thermal parameters*

$RU_{ij} = \sum U(X)_{ij} \times U(N)_{ij}/\sum U(N)_{ij}^2$, where the sum extends over all non-hydrogen atoms.

Procedure	RU_{11}	RU_{22}	RU_{33}	RU_{12}	RU_{13}	RU_{23}
1	0·927	0·959	0·859	0·978	0·863	0·996
2	0·929	0·961	0·863	0·966	0·860	0·983
3	0·931	0·958	0·867	0·959	0·864	0·977
4	0·931	0·955	0·870	0·949	0·859	0·964
5	0·915	0·979	0·850	1·011	0·884	1·045
6	0·929	0·959	0·858	0·974	0·860	0·988
7	0·932	0·962	0·863	0·975	0·863	0·986

Table 6. P—O *bond distances* (Å)

Bond	X-ray refinements 1	2	3	4	5	Neutron
P—O(1)	1·5056 (6)	1·5052 (6)	1·5049 (7)	1·5050 (8)	1·5064 (9)	1·5030 (13)
P—O(2)	1·5198 (6)	1·5197 (6)	1·5190 (7)	1·5192 (9)	1·5212 (8)	1·5190 (11)
P—O(3)	1·5607 (7)	1·5610 (7)	1·5607 (8)	1·5618 (11)	1·5611 (9)	1·5595 (12)
P—O(4)	1·5754 (6)	1·5751 (6)	1·5747 (7)	1·5753 (9)	1·5767 (18)	1·5745 (11)

DOCKET ALARM

Explore Litigation Insights

Docket Alarm provides insights to develop a more informed litigation strategy and the peace of mind of knowing you're on top of things.

Real-Time Litigation Alerts

Keep your litigation team up-to-date with **real-time alerts** and advanced team management tools built for the enterprise, all while greatly reducing PACER spend.

Our comprehensive service means we can handle Federal, State, and Administrative courts across the country.

Advanced Docket Research

With over 230 million records, Docket Alarm's cloud-native docket research platform finds what other services can't. Coverage includes Federal, State, plus PTAB, TTAB, ITC and NLRB decisions, all in one place.

Identify arguments that have been successful in the past with full text, pinpoint searching. Link to case law cited within any court document via Fastcase.

Analytics At Your Fingertips

Learn what happened the last time a particular judge, opposing counsel or company faced cases similar to yours.

Advanced out-of-the-box PTAB and TTAB analytics are always at your fingertips.

API

Docket Alarm offers a powerful API (application programming interface) to developers that want to integrate case filings into their apps.

LAW FIRMS
Build custom dashboards for your attorneys and clients with live data direct from the court.

Automate many repetitive legal tasks like conflict checks, document management, and marketing.

FINANCIAL INSTITUTIONS
Litigation and bankruptcy checks for companies and debtors.

E-DISCOVERY AND LEGAL VENDORS
Sync your system to PACER to automate legal marketing.

WHAT WILL YOU BUILD? | **sales@docketalarm.com** | **1-866-77-FASTCASE**

fastcase® Smarter legal research.